Arnold Schwarzenegger
Governor

THERMAL CALIBRATION OF THE WINDOWS TESTBED FACILITY

PIER FINAL PROJECT REPORT

Prepared For:
California Energy Commission
Public Interest Energy Research Program

Prepared By:
Lawrence Berkeley National Laboratory

ERNEST ORLANDO LAWRENCE
BERKELEY NATIONAL LABORATORY

May 2006
CEC-500-2006-052-AT10

Prepared By:
Lawrence Berkeley National Laboratory
Eleanor Lee
Berkeley, California
Contract No. 500-01-023

Prepared For:
California Energy Commission
Public Interest Energy Research (PIER) Program

Chris Scruton
Contract Manager

Ann Peterson
Building End-Use Efficiency Team Leader

Nancy Jenkins
PIER Energy Efficiency Research Office Manager

Martha Krebs, Ph.D.
Deputy Director
ENERGY RESEARCH AND DEVELOPMENT DIVISION

B. B. Blevins
Executive Director

DISCLAIMER

This report was prepared as the result of work sponsored by the California Energy Commission. It does not necessarily represent the views of the Energy Commission, its employees or the State of California. The Energy Commission, the State of California, its employees, contractors and subcontractors make no warrant, express or implied, and assume no legal liability for the information in this report; nor does any party represent that the uses of this information will not infringe upon privately owned rights. This report has not been approved or disapproved by the California Energy Commission nor has the California Energy Commission passed upon the accuracy or adequacy of the information in this report.

Acknowledgments

This work was supported by the California Energy Commission through its Public Interest Energy Research (PIER) Program on behalf of the citizens of California and by the Assistant Secretary for Energy Efficiency and Renewable Energy, Office of Building Technology, State and Community Programs, Office of Building Research and Standards of the U.S. Department of Energy under Contract No. DE-AC02-05CH11231.

We are indebted to Chris Scruton and Nancy Jenkins of the California Energy Commission and Marc LaFrance of the US Department of Energy for their invaluable guidance, enthusiasm, and support throughout this multiyear project. We would also like to thank the following members of our Project Advisory Committee for taking the time to provide insightful technical and market-related input into the direction of this R&D:

Carl Wagus	American Architectural Manufacturers Association
Thomas Guarr	Gentex Corporation
Jan Berman	Mechoshade Systems, Inc.
Grant Brohard	Pacific Gas & Electric Company
Charles Hayes	SAGE Electrochromics, Inc.
Micheal Myser	SAGE Electrochromics, Inc.
John Durschinger	Skidmore, Owings & Merrill LLP
Gregg Ander	Southern California Edison
Hula Demiryont	Sytecorp
Kevin Settlemyre	The Green Roundtable, Inc.
Glenn Hughes	The New York Times
David Thurm	The New York Times
Mark Levi	US General Services Administration
Thomas Mifflin	Wausau Window and Wall Systems

Thomas Mifflin of Wausau Window and Wall Systems provided enthusiastic and dedicated guidance, engineering support, and materials for our electrochromic field test facility's curtainwall system without which this project probably would not have gotten off the ground. SAGE Electrochromics, Inc. also remained dedicated throughout the duration of this project, providing technical assistance and product revisions to meet our demanding project requirements.

The project team consisted of staff from a variety of disciplines within the Environmental Energy Technologies Division at the Lawrence Berkeley National Laboratory:

Andre Anders, Ph.D., Material Scientist, Thin Film Coatings
Zachery Apte, IR Laboratory Tests
Robert Clear, Ph.D., Human Factors, Statistical Analysis
Dennis DiBartolomeo, Systems Engineering, Field Test Operations
Luis Fernandes, Ph.D., Radiance Mathematica Optimizations
Daniel Fuller, Testbed Networking and Communications
Howdy Goudey, IR Laboratory Tests, Curtainwall Engineering, Sensors and Instrumentation
Chuck Hambelton, Curtainwall Engineering, Sensors and Instrumentation
Philip Haves, Ph.D., Commercial Building Systems, HVAC Interactions
Vorapat Inkarojrit, Ph.D., Human Factors, High-Dynamic-Range Digital Imaging
Joseph Klems, Ph.D., Heat Flow Monitoring and Thermal Analysis

Christian Kohler, Window Modeling, Testbed Networking and Communications
Judy Lai, Radiance Modeling
Eleanor Lee, Co-Principal Investigator
Steve Marsh, Curtainwall Engineering, Sensors and Instrumentation
Robin Mitchell, Window Modeling
Thomas Richardson, Ph.D., Material Scientist, Electrochromics
Micheal Rubin, Ph.D., Material Scientist, NFRC
Francis Rubinstein, Lighting Controls, IBECS Networking and Controls
Stephen Selkowitz, Principal Investigator
Charles Taberski, Facilities Management, Testbed Facility Engineering and Construction
Duo Wang, Data Analysis
Peng Xu, Ph.D., Commercial Building Systems, HVAC Interactions
Mehry Yazdanian, Heat Flow and Data Analysis

And colleagues from other institutions and companies:
Ren Andersen, Ph.D., National Renewable Energy Laboratory
Oyvind Aschehoug, Ph.D., Visiting Professor, Norwegian University of Science and Technology, Trondheim
Thibaut Falcon, École Nationale des Travaux Publics de l'État, Field Testing and Instrumentation
Lixing Gu, Ph.D., Florida Solar Energy Center, Testbed Facility Engineering
Aslihan Tavil, Faculty of Architecture, Istanbul Technical University, Turkey
Greg Ward, Anyhere Software, Radiance Mathematica Optimizations, High-Dynamic-Range Digital Imaging

Citation: Klems, J. 2004. Thermal calibration of the windows testbed facility. Technical report.

Preface

The Public Interest Energy Research (PIER) Program supports public interest energy research and development that will help improve the quality of life in California by bringing environmentally safe, affordable, and reliable energy services and products to the marketplace.

The PIER Program, managed by the California Energy Commission (Commission), annually awards up to $62 million to conduct the most promising public interest energy research by partnering with Research, Development, and Demonstration (RD&D) organizations, including individuals, businesses, utilities, and public or private research institutions.

PIER funding efforts are focused on the following six RD&D program areas:

- Buildings End-Use Energy Efficiency
- Industrial/Agricultural/Water End-Use Energy Efficiency
- Renewable Energy
- Environmentally-Preferred Advanced Generation
- Energy-Related Environmental Research
- Energy Systems Integration

What follows is an attachment to the final report for the Advancement of Electrochromic Windows project, Contract Number 500-01-023, conducted by the Lawrence Berkeley National Laboratory, Berkeley, CA. This project contributes to the PIER Building End-Use Energy Efficiency program.

This attachment, "Advancement of Electrochromic Windows: Journal and Technical Reports" (Attachment A-1), provides supplemental information to the project's final report and includes journal and technical reports related to the following three subjects:

- *Systems Engineering*
- *Performance Impacts*
- *Information Resources*

For more information on the PIER Program, please visit the Commission's Web site at: http://www.energy.ca.gov/research/index.html or contact the Commission's Publications Unit at 916-654-5200.

Abstract

The technical report documents the thermal calibration of the LBNL Windows Testbed Facility, which was used to quantify the thermal effects due to solar heat gains of electrochromic windows in comparison to a reference window.

This is part of a set of attachments to the "Advancement of Electrochromic Windows: Journal and Technical Reports" document, produced by the Advancement of Electrochromic Windows project, funded by the California Energy Commission's Public Interest Energy Research (PIER) Program and the U.S. Department of Energy. See the CEC PIER website for more information about this project or visit:

http://windows.lbl.gov/comm_perf/Electrochromic/electroSys-cec.htm

Table of Contents

I. Calibrating the Testbed Facility **1**

Problem Statement **1**

Heating and Cooling Efficiencies *1*

Overall Heat Balance *2*

Chamber Temperature Corrections 2

Shell Corrections 4

Corrections due to Variations in Guard Temperature 4

Corrections for Chamber Air Flow Rate 5

Corrections for Solar Transmittance and Lighting Power Level 5

Corrections for Differences in Chamber Construction 7

II. Thermal Calibration Tests **9**

Static Tests **9**

Dynamic Tests (Nighttime) **11**

Solar Tests (Daytime/Weekend) **11**

III. Analysis of Thermal Calibration Tests **13**

Static Tests **13**

Definition of Time Average *13*

Cooling & Heating System Efficiency (Tests 4 &5) *13*

Cooling System Efficiency (Test 4) 14

Heating System Efficiency (Test 5) 15

Floor, Exterior Wall, and Window UA Values (Tests 1 and 3) *16*

Ceiling & Interior Wall UA Values (Test 2) *17*

Sensitivity To Changes in Static Conditions (Tests 6,7 and 8) *17*

Dynamic Tests **19**

Chamber Temperature Ramp (Test D1) *19*

Control System Response (Test D2) *21*

Radiant Heater Pulse Test (D3) *22*

Lighting Pulse (Test D4) *22*

Radiant and Light Losses Through Window (Tests D5, D6) *22*

Application of the Corrections **23**

IV. Thermal Calibration Results **24**

Introduction **24**

Steady-State Correction Model **24**

Fits to The Static Test Data **25**

Determination of the Heating and Cooling Calibration Constants **26**

Nomenclature **37**

References **38**

I. Calibrating the Testbed Facility

Problem Statement

In a typical test bed measurement, test window systems will be mounted in each test chamber and controlled in some manner to provide an interior lighting environment desired in each test room. The windows and control strategies may differ among the three test chambers. For each test room, denoted by μ, the lighting power L_{μ}, the cooling power extracted, $P_{C\mu}$, and the heating power added, $P_{H\mu}$, are measured and averaged over some time period, yielding the average quantities of interest:

$$\left\langle \mathrm{L}_{\mu} \right\rangle \text{ and } \left\langle P_{C\mu} - P_{H\mu} \right\rangle$$

If one performs a test comparing windows and daylighting strategies in a pair of the chambers, μ and ν, resulting in measured differences

$$\Delta \mathcal{L}_{\mu\nu} = \left\langle \mathcal{L}_{\mu} - \mathcal{L}_{\nu} \right\rangle$$

and

$$\Delta P_{\mu\nu} = \left\langle \left(P_{C\mu} - P_{H\mu}\right) - \left(P_{C\nu} - P_{H\nu}\right) \right\rangle$$

then what corrections must be applied to $\Delta P_{\mu\nu}$ to account for those differences in energy flows between the two chambers that are not through the window, and do not result from differences in the applied lighting power?

Heating and Cooling Efficiencies

In general, there may be heat losses or gains between the heating/cooling equipment plenum and the supply/return ducts, with the result that only a fraction ε of the applied heating or cooling power actually reaches the space. This fraction could differ between the heating and cooling system, and between rooms. Accordingly, the actual difference in power usage between rooms will be

$$\Delta P \equiv \left(\Delta P_{\mu\nu}\right)_{True} = \left\langle \left(\varepsilon_{C\mu} P_{C\mu} - \varepsilon_{H\mu} P_{H\mu}\right) - \left(\varepsilon_{C\nu} P_{C\nu} - \varepsilon_{H\nu} P_{H\nu}\right) \right\rangle$$

In general, in the remainder of this document we shall use the symbol P_{μ} to denote the true power applied to chamber μ, implicitly assuming the "True" subscript; that is

$$P_{\mu} = \left(\varepsilon_{C\mu} P_{C\mu} - \varepsilon_{H\mu} P_{H\mu}\right) ,$$

where $P_{C\mu}$ and $P_{H\mu}$ are the *measured* cooling and heating powers.

Overall Heat Balance

For a test chamber, μ, holding a window, ω, with applied heating, cooling and lighting powers as denoted above, and exposed to an incident solar flux, *S*, the overall heat balance of the test room (air) is given by

$$\Delta P = Q_{C\omega}(\mathcal{A}_\omega(\theta)S, T_\mu, T_o) + \sum_k Q_{C\mu k}(\mathcal{L}_\mu, \mathcal{T}_\omega(\theta)S, T_\mu, T_o, T_G) + Q_{C\mathcal{L}}(\mathcal{L}_\mu) \ , \qquad (1)$$

where

T_μ	is the chamber air temperature
T_o	is the outdoor air temperature
T_G	is the guard temperature
$Q_{C\omega}$	is the convective part of the window heat flow
$Q_{C\mu k}$	is the convective part of the surface heat flow for (non-window) surface k
$Q_{C\mathcal{L}}$	is the convective heat flow from the lights
θ	is the solar incident angle
$\mathcal{T}_\omega$	is the instantaneous window solar transmittance X effective area
$\mathcal{A}_\omega$	is the instantaneous window solar absorptance X effective area
$\varepsilon_{C\mu}$	is the cooling system efficiency
$\varepsilon_{H\mu}$	is the heating system efficiency
S	is the (instantantaneous) incident solar flux

All of the convective heat flows are defined as positive flowing into the chamber air.

The convective part of the window heat flow results from a straightforward heat balance, since thermal storage in the window can be neglected. The amount of solar energy (per unit area) absorbed by the window, the interior and exterior convective and radiative coefficients, the window construction, and the interior and exterior air and radiant temperatures together determine the interior and exterior surface temperatures of the window; the former together with the interior air temperature and the window area then determine $Q_{C\omega}$.

Similarly, the convective heat flow from the lights results from an instantaneous heat balance between the light source and the chamber air.

In general, the temperatures of the chambers may be different during a given test, due to limitations in the control systems. In addition, L , $\mathcal{T}_\omega$, and $\mathcal{A}_\omega$ will all be different (this is the point of the test).

Chamber Temperature Corrections

We assume differences in chamber temperature are sufficiently small that we can expand equation 1 and drop higher-order terms.

$$d(\Delta P) = \frac{d(\Delta P)}{dT_\mu} \cdot \langle T_\mu - T_R \rangle - \frac{d(\Delta P)}{dT_\nu} \cdot \langle T_\nu - T_R \rangle \ ,$$

where T_R is some chosen standard chamber temperature, and

$$\frac{d(\Delta P)}{dT_\mu} = \frac{dQ_{C\omega}}{dT_\mu} + \sum_k \frac{dQ_{C\mu k}}{dT_\mu} \quad . \tag{2}$$

For the window the thermal time response can be neglected, so that

$$\frac{dQ_{C\omega}}{dT_\mu} = -A_{T\mu} \cdot U_{\omega_\mu} \ .$$

The non-window heat flows can be calculated from the standard response factor series,

$$Q_{\mu k}(t) = A_{\mu k} \sum_{n=0}^{\infty} \left[Y_{\mu kn} \cdot \left(T_{E(k)}(t - n\delta) - T_{00} \right) - Z_{\mu kn} \cdot \left(T_{Sk}(t - n\delta) - T_{00} \right) \right] , \tag{3}$$

where $Q_{\mu k}(t)$ is the heat flow out of surface k (negative value for heat flow into the surface), $A_{\mu k}$ is the area of surface k, $Y_{\mu kn}$ and $Z_{\mu kn}$ are the standard cross-surface and same-surface response factors for surface k (n=1, 2, …), $T_{E(k)}$ is the exterior air temperature for surface k (either T_o or T_G, depending on the surface), T_{Sk} is the surface temperature for surface k, δ is the time interval for the response-factor temperature history, and T_{00} is an arbitrary reference temperature. The chamber index μ is included to identify quantities that may differ between chambers.
Note that

$$Q_{\mu k}(t) = Q_{C\mu k}(t) + Q_{R\mu k}(t) \ ,$$

where $Q_{R\mu k}(t)$ is the radiative heat flux at the surface.

If we can assume that the differences in chamber temperature are slowly varying compared to the chamber response time, then all the terms in the second part of the series change together, and

$$\frac{dQ_{C\mu k}}{dT_\mu} = -A_{\mu k} \cdot U_{\mu k} \ .$$

Whether this assumption is correct is an empirical question, to be settled when the chambers are operated. If it does not hold then this analysis becomes considerably more complicated.
The quantities U_{ω_μ} and $U_{\mu k}$ implicitly contain the effects of radiant interchanges among the interior surfaces, and so are not really properties of the individual constructions. In

particular, $U_{\mu k}$ is not the sum of the response factors in equation 3 (which are defined with respect to the interior surface temperatures). Combining these equations, the change in the corrected average power difference is (assuming slow changes of chamber temperature with time)

$$\begin{aligned} d(\Delta P) = & \left(A_{T\omega_\nu} \cdot U_{\omega_\nu} + \sum_k A_{\nu k} \cdot U_{\nu k} \right) \cdot \langle T_\nu - T_R \rangle \\ & - \left(A_{T\omega_\mu} \cdot U_{\omega_\mu} + \sum_k A_{\mu k} \cdot U_{\mu k} \right) \cdot \langle T_\mu - T_R \rangle \end{aligned} \tag{4}$$

This quantity must of course be subtracted from the measured value of ΔP.

Shell Corrections

For notational simplicity we term the above chamber corrections "shell" corrections, since they pertain to the thermal shell of each test chamber. We define

$$\mathbf{S}_\mu^\omega = A_{T\omega_\mu} \cdot U_{\omega_\mu} \tag{5a}$$

for the window in chamber μ,

$$\mathbf{S}_\mu^F = \sum_{k=\,floor,extwall} A_{\mu k} \cdot U_{\mu k} \tag{5b}$$

for the floor and exterior walls, and

$$\mathbf{S}_\mu^G = \sum_{k\neq\,floor,extwall} A_{\mu k} \cdot U_{\mu k} \tag{5c}$$

for those portions of the chamber envelope adjacent to the interior guard. Then in terms of these quantities equation 4 becomes

$$\begin{aligned} d(\Delta P) = & \left(\mathbf{S}_\mu^\omega + \mathbf{S}_\mu^F + \mathbf{S}_\mu^G \right) \cdot \langle T_R - T_\mu \rangle \\ & - \left(\mathbf{S}_\nu^\omega + \mathbf{S}_\nu^F + \mathbf{S}_\nu^G \right) \cdot \langle T_R - T_\nu \rangle \end{aligned} \tag{4a}$$

Corrections due to Variations in Guard Temperature

It is possible that the guard temperature could be different for different chambers, due to spatial gradients in guard temperature. This correction is derived in the same way as the corrections for room temperature, except that they involve only those chamber surfaces whose opposite sides face the guard:

$$d(\Delta P)=\left(\sum_{k\neq floor,extwall} A_{\mu k}\cdot U_{\mu k}\right)\cdot\left\langle T_{G\mu}-T_{G0}\right\rangle-\left(\sum_{k\neq floor,extwall} A_{\nu k}\cdot U_{\nu k}\right)\cdot\left\langle T_{G\nu}-T_{G0}\right\rangle \tag{6}$$

Here $T_{G\mu}$ and $T_{G\nu}$ are the local guard temperatures adjacent to chambers μ and ν, respectively, and T_{G0} is the standard reference guard temperature.
In terms of the shell corrections, equation 6 becomes,

$$d(\Delta P)=\mathbf{S}_{\mu}^{G}\cdot\left\langle T_{G\mu}-T_{G0}\right\rangle-\mathbf{S}_{\nu}^{G}\cdot\left\langle T_{G\nu}-T_{G0}\right\rangle \tag{6a}$$

Corrections for Chamber Air Flow Rate

Both $Q_{C\omega}$ and $Q_{C\mu k}$ may implicitly depend on the air circulation rate, f, in the chambers. This is because both the window and envelope U-factors and the interior surface temperatures in equation 3 depend on the interior surface heat transfer coefficients, which may depend on f. The resulting variation in the power difference is

$$d(\Delta P)=\left(\frac{dQ_{C\omega_\mu}}{df_\mu}+\sum_k\frac{dQ_{C\mu k}}{df_\mu}\right)\left\langle f_\mu-f_0\right\rangle-\left(\frac{dQ_{C\omega_\nu}}{df_\nu}+\sum_k\frac{dQ_{C\nu k}}{df_\nu}\right)\left\langle f_\nu-f_0\right\rangle\ , \tag{7}$$

where f_μ and f_ν represent the actual air recirculation rate in chamber μ and ν, respectively, f_0 is the standard reference recirculation rate, ω_μ denotes the window in chamber μ, and ω_ν the window in chamber ν. There is no simple way to calculate the derivatives in equation 7. They must be measured empirically.
We simplify the notation of equation 7 by defining a flow correction factor, $\mathbf{F}$, for each chamber:

$$\mathbf{F}_\mu=\frac{dQ_{C\omega_\mu}}{df_\mu}+\sum_k\frac{dQ_{C\mu k}}{df_\mu} \tag{8}$$

Then equation 7 becomes

$$d(\Delta P)=\mathbf{F}_\mu\cdot\left\langle f_\mu-f_0\right\rangle-\mathbf{F}_\nu\cdot\left\langle f_\nu-f_0\right\rangle \tag{7a}$$

Corrections for Solar Transmittance and Lighting Power Level

Changes in either the lighting power or solar transmittance (and absorbtance) will cause changes in $Q_{C\omega}$ (in the case of solar) or Q_{CL} (in the case of lighting), but these changes are part of the effect to be measured. However, there will also be changes in $Q_{C\mu k}$.
Whether these changes are also part of the signal to be measured is a matter of interpretation; however, knowing the effect of these changes will be relevant to discussion below, regardless of interpretation, so we proceed to develop them.

Changes in $Q_{C\mu k}$ occur because changes in either the lighting level or the solar transmittance of the window change the radiant flux incident on the interior surfaces. This change causes in turn a change in the surface temperatures and heat flows in equation 3. This in turn causes a change in the convective heat flow from the surface. As equation 3 indicates, we must examine the change in surface temperature at each time, $t - n\delta$, caused by a change in lighting level at that time:

$$dT_{Skn} \equiv dT_{Sk}(t - n\delta) = \frac{\partial T_{Sk}(t - n\delta)}{\partial \mathrm{L}} \Delta \mathrm{L}(t - n\delta) \equiv \frac{\partial T_{Sk\mu n}}{\partial \mathrm{L}} \Delta \mathrm{L}_{\mu \mathrm{n}} \tag{9a}$$

where in the notation on the extreme left and right we have indicated the time dependence by the subscript n (i.e., implying $t - n\delta$, where t is the current time) and have added a subscript μ to denote the chamber (which will be needed below). Similarly, a change in the surface temperature can result from a change in the window solar transmittance, but here both the transmittance and the incident solar flux are time dependent:

$$dT_{Skn} \equiv dT_{Sk}(t - n\delta) = \frac{\partial T_{Sk}(t - n\delta)}{\partial \left(\mathcal{T}_{\omega}(\theta) S\right)} \Delta \mathcal{T}_{\omega}(\theta, t - n\delta) S(t - n\delta) \equiv \frac{\partial T_{Sk\mu n}}{\partial \left(\mathcal{T}_{\omega}(\theta) S\right)} \Delta \mathcal{T}_{\omega_{\mu} n} S_n \tag{9b}$$

We must consider that $Q_{C\mu k}$ is implicitly a function of each of the temperature changes in the time series of equation 3:

$$d(\Delta P) = \sum_k \left(\left\langle \sum_n \frac{\partial Q_{C\mu k}}{\partial T_{Skn}} dT_{S\mu kn} \right\rangle - \left\langle \sum_n \frac{\partial Q_{C\nu k}}{\partial T_{Skn}} dT_{S\nu kn} \right\rangle \right) \tag{10}$$

where again chamber-distinguishing subscripts have been added. The computation of the average is complicated by the fact that the changes in surface temperature at each time are interrelated by equation 3 and the requirement of a net heat balance for each surface at each time.

Substituting equation 9a into equation 10 yields

$$d(\Delta P) = \sum_k \left(\left\langle \sum_n \frac{\partial Q_{C\mu k}}{\partial T_{Skn}} \frac{\partial T_{Sk\mu n}}{\partial \mathrm{L}} \Delta \mathrm{L}_{\mu \mathrm{n}} \right\rangle - \left\langle \sum_n \frac{\partial Q_{C\nu k}}{\partial T_{Skn}} \frac{\partial T_{Sk\nu n}}{\partial \mathrm{L}} \Delta \mathrm{L}_{\nu \mathrm{n}} \right\rangle \right) \tag{11}$$

if we consider the portion of this equation due to one of the two chambers,

$$d(P_{\mu}) = \sum_k \left\langle \sum_n \frac{\partial Q_{C\mu k}}{\partial T_{Skn}} \frac{\partial T_{Sk\mu n}}{\partial \mathrm{L}} \Delta \mathrm{L}_{\mu \mathrm{n}} \right\rangle = \left\langle \sum_n \left(\sum_k \frac{\partial Q_{C\mu k}}{\partial T_{Skn}} \frac{\partial T_{Sk\mu n}}{\partial \mathrm{L}} \right) \Delta \mathrm{L}_{\mu \mathrm{n}} \right\rangle \equiv \mathcal{V}_{\mu}^{L} \left\langle \Delta \mathrm{L}_{\mu} \right\rangle \tag{12}$$

which defines the average correction, $\mathcal{V}_{\mu}^{L}$, due to a change in lighting power level. In terms of this correction, equation 11 then becomes

$$d(\Delta P) = \mathcal{V}_{\mu}^{L}\left\langle \Delta\mathcal{L}_{\mu}\right\rangle - \mathcal{V}_{\nu}^{L}\left\langle \Delta\mathcal{L}_{\nu}\right\rangle \quad . \tag{13}$$

Similarly, substituting equation 9b into equation 10 gives

$$d(\Delta P) = \sum_{k}\left(\left\langle \sum_{n}\frac{\partial Q_{C\mu k}}{\partial T_{Skn}}\frac{\partial T_{Sk\mu n}}{\partial\left(\mathcal{T}_{\omega}(\theta)S\right)}\Delta\mathcal{T}_{\omega_{\mu}n}S_{n}\right\rangle - \left\langle \sum_{n}\frac{\partial Q_{C\nu k}}{\partial T_{Skn}}\frac{\partial T_{Sk\nu n}}{\partial\left(\mathcal{T}_{\omega}(\theta)S\right)}\Delta\mathcal{T}_{\omega_{\nu}n}S_{n}\right\rangle\right), \tag{14}$$

and considering each chamber separately, we define

$$d(P_{\mu}) = \sum_{k}\left\langle \sum_{n}\frac{\partial Q_{C\mu k}}{\partial T_{Skn}}\frac{\partial T_{Sk\mu n}}{\partial\left(\mathcal{T}_{\omega}(\theta)S\right)}\Delta\mathcal{T}_{\omega_{\mu}n}S_{n}\right\rangle = \left\langle \sum_{n}\left(\sum_{k}\frac{\partial Q_{C\mu k}}{\partial T_{Skn}}\frac{\partial T_{Sk\mu n}}{\partial\left(\mathcal{T}_{\omega}(\theta)S\right)}\right)\Delta\mathcal{T}_{\omega_{\mu}n}S_{n}\right\rangle$$

Defining

$$\mathcal{V}_{\mu n}^{S} \equiv \sum_{k}\frac{\partial Q_{C\mu k}}{\partial T_{Skn}}\frac{\partial T_{Sk\mu n}}{\partial\left(\mathcal{T}_{\omega}(\theta)S\right)} \tag{15}$$

Then we have

$$d(P_{\mu}) = \left\langle \sum_{n}\mathcal{V}_{\mu n}^{S}\Delta\mathcal{T}_{\omega_{\mu}n}S_{n}\right\rangle \equiv \mathcal{V}_{\mu}^{S}\left\langle \Delta\mathcal{T}_{\omega_{\mu}}S\right\rangle \tag{16}$$

which defines the average correction, $\mathcal{V}_{\mu}^{S}$, due to a change in transmitted solar energy. Equation 16 then becomes

$$d(\Delta P) = \mathcal{V}_{\mu}^{S}\cdot\left\langle \Delta\mathcal{T}_{\omega_{\mu}}S\right\rangle - \mathcal{V}_{\nu}^{S}\cdot\left\langle \Delta\mathcal{T}_{\omega_{\nu}}S\right\rangle \tag{17}$$

Corrections for Differences in Chamber Construction

The corrections for guard and chamber temperature differences above do not account for differences in chamber construction. If these exist, then there will be differences in the chamber power consumptions even under identical interior and exterior conditions. A likely special case is differences in the UA values of the window systems being tested. The simplest correction for these effects is a U-factor one.

For the windows,

$$d(\Delta P) = \left(A_{T\omega_{\mu}}\cdot U_{\omega_{\mu}} - A_{T\omega_{\nu}}\cdot U_{\omega_{\nu}}\right)\left\langle T_{o} - T_{R}\right\rangle = \left(\mathbf{S}_{\mu}^{\omega} - \mathbf{S}_{\nu}^{\omega}\right)\left\langle T_{o} - T_{R}\right\rangle \tag{18}$$

For the interior walls,

$$d(\Delta P) = \left(\sum_{k \neq floor, extwall} \left(A_{\mu k} \cdot U_{\mu k} - A_{\nu k} \cdot U_{\nu k} \right) \right) \cdot \langle T_{G0} - T_R \rangle = \left(\mathbf{S}_{\mu}^{G} - \mathbf{S}_{\nu}^{G} \right) \cdot \langle T_{G0} - T_R \rangle \qquad (19)$$

And for the floor and exterior walls,

$$d(\Delta P) = \left(\sum_{k = floor, extwall} \left(A_{\mu k} \cdot U_{\mu k} - A_{\nu k} \cdot U_{\nu k} \right) \right) \cdot \langle T_o - T_R \rangle = \left(\mathbf{S}_{\mu}^{F} - \mathbf{S}_{\nu}^{F} \right) \cdot \langle T_o - T_R \rangle \qquad (20)$$

The validity of the correction in equation 20 must be checked empirically to verify that the averaging period is sufficiently long compared to the exterior wall, floor time response. If this is not the case a more elaborate correction method must be utilized.

II. Thermal Calibration Tests

Static Tests

These tests should be conducted at nighttime. For each test all three test chambers ("chamber") should be set up to run identical conditions, with any furniture planned for the lighting tests in place. (Note: all of the environmental temperatures used in these tests are within the 40ºF-90ºF (4.4ºC-32ºC) temperature range allowed by the equipment specifications.)

0. **Baseline Tests:** As part of normal operation of the chamber, obtain data for a number of nights with conditions normal and the chamber temperatures at 21ºC. General climatic conditions should be similar to those of the calibration tests. (If different calibration tests are made at widely separated times, then some baseline data should be obtained during the same general time (i.e., same general climatic conditions) as each calibration test.
1. **Interior temperature sweep:** Interior chamber air temperature setpoint: 11º C, 21º C, 31ºC (if 11ºC and/or 31ºC are not attainable, then use 16ºC and/or 26ºC); 1 night at each setting. Guard/control room temperature should be set at the same temperature as the chambers. No lights in chambers.
2. **Guard temperature sweep:** Prior to these tests the average nighttime outdoor temperature should be determined. The chamber interior air temperature setpoint of all three chambers should be set as close to this temperature as possible. Guard temperature setpoint: 11ºC, 21ºC, 31ºC (same qualifications as above); 1 night per setting. No lights in chambers.
3. **Insulated window:** Cover the windows in each chamber with 1 inch expanded polystyrene ("blue foam", nominal R-4 or R-5) insulation (EPS). Insulation should be mounted on the inside, and should cover both glazings and frames. Repeat test 1 in this configuration.
4. **Cooling system efficiency:** Obtain 3 approximately 1500W electric convective heaters (circulating hot water or oil, no fan—SoftHeat or something similar). Pre-adjust them so that they draw equal power (or arrange with a variac or some form of series resistor in the room). Place a heater in each chamber, in the center of the room, well off the floor. Run with one heater in each chamber at equal power, approx 1500W. Chamber temperature setting ,21º C; 1 night. No lights in chambers.
5. **Heating system efficiency:** Set the minimum on the cooling fan to force the system into a cool and reheat mode. Adjust the cooling rate until the heater power is approximately 2KW, and fix the cooling rate at this value. Run system for 4 hours (?) in this mode, then switch on 1500W heaters and run for the remainder of the night.
6. **Radiant temperature sensitivity:** Get 3 quartz radiant heaters (w/o fans). Pre-match the power levels of the three heaters, as with the convective heaters. If they

are not constructed so that the radiant energy comes out in only one hemisphere, make and arrange a reflective shield such that the window will be shadowed from radiant energy. Suspend each heater so that it is at least 2 ft from the window, at about the level of the lights or a bit lower, and oriented so that the radiant energy strikes the floor and as much of the lower walls as necessary, but not the window. With the chamber (and guard) temperature set point at 21ºC, run the heater at 1500W for 1 night.

7. **Lighting power:** With the guard and chamber temperature set points at 21ºC and all other conditions normal, run for one night with the lights at full power. Repeat this test for a second night with the windows covered with 1in EPS insulation.
8. **Air Flow sensitivity:** Run for 1 night with the guard and chamber temperature set point at 21ºC. Then repeat test 6 for 1 night with the air flow rate reduced to half its normal value. Prior to this test, check for stability of the control; if the system is unable to maintain a stable room temperature with the 1500W heater on, try a higher air flow rate, up to 75% of the normal flow. If the control is still inadequate at 75% flow, then reduce the heater power until stable control is obtained. Run the test under these conditions. The heater powers will need to be rechecked to insure that the power level is the same in each chamber. It is assumed that adjusting the heater thermostat switch will vary the duty factor of the quartz heater. The on and off times of the heater should be determined, and one should verify that the measured average power corresponds to a large enough number of cycles to assure that the power level settings are the same before initiating the test. (These considerations also apply to test 6.)

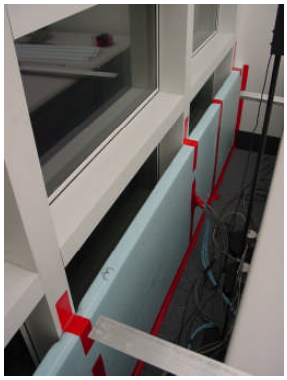

Left: Detail of foam wall that was applied to entire 10x11 ft window wall in all three chambers; middle: radiant heater pulse test with insulated window; right: convective heater pulse test (conducted at night) used to determine cooling system efficiency.

Dynamic Tests (Nighttime)

1. **Chamber temperature ramp:** Run the chambers at 21ºC until midnight. At that time, increase each chamber temperature set point by 0.2ºC each minute until 12:30AM. Then decrease the set point by the same amount each minute until it is again at 21ºC. Continue at this set point for the rest of the night.
2. **Convective heater pulse:** Set up as for static test 4 (cooling system efficiency), but rig the heaters with a timer that turns them on only for one hour beginning at 12AM. Run 1 night.
3. **Radiant heater pulse:** Set up as for static test 6 (radiant temperature sensitivity), but with the quartz heaters rigged on a timer as in dynamic test 2 above. Radiant heater to go on for one hour beginning at 12AM. Run 1 night.
4. **Lighting pulse:** Set up as for static test 7, but only switch the lights on (at full power) for one hour beginning at 12AM. Run 1 night.
5. **Radiant heater pulse with insulated window:** Repeat dynamic test 3 with the window (including frame) covered with 1-inch EPS foam. The inner side of the foam should be covered with aluminum foil.
6. **Lighting pulse with insulated window:** Repeat dynamic test 4 with the window (including frame) covered with 1-inch EPS foam. The inner side of the foam should be covered with aluminum foil.

Solar Tests (Daytime/Weekend)

1. **Equal glazing transmittance comparison:** Set the glazing system with the lowest maximum solar transmittance to its maximum value, and adjust those in the other test chambers to have equal transmittance. Check for equality by measuring the transmitted solar intensity through each glazing panel with a pyranometer to verify that the transmittances are equal (to within 2%). With all the chamber temperatures set a normal conditions and lights off, run for a minimum of 24 hours (preferably a weekend) with this setting.
2. **Equal weighted transmittance comparison:** Using sun trajectories for the expected test period, calculate the effective unshaded glazing area for the SAGE and Flabeg windows averaged over the several hours of largest incident beam solar. Use this to calculate the relative transmittance settings for the two windows that will give an equal area-weighted transmittance averaged over these hours. This is defined as an "equal weighted transmittance". With all the chamber temperatures set at normal conditions, adjust the electrochromic settings to give the maximum transmission compatible with equal weighted transmittance. Run for a minimum of 24 hours (preferably a weekend) with this setting.
3. **Absorbing floor test:** Place a floor solar interception system (FSIS, described/designed elsewhere) with a black coating on the portion of the floor in each chamber expected to receive beam solar energy. Set up all other conditions as in solar test 2. Run for 1 24-hour period, minimum. (Or a weekend.)
4. **Reflecting floor test:** Repeat solar test 3 with a highly diffusely reflecting white coating on the FSIS.

5. **Absorbing sill/frame test:** With the same setup as solar test 3, insert a window solar interception system (WSIS, described/designed elsewhere) with a black coating in each glazing section in all three chambers. Run for 1 24-hour period, minimum.
6. **Reflecting sill/frame test:** With the same setup as solar test 4, insert a window solar interception system (WSIS, described/designed elsewhere) with a highly diffusely reflecting white coating in each glazing section in all three chambers. Run for 1 24-hour period, minimum.

III. Analysis of Thermal Calibration Tests

Static Tests

Definition of Time Average

A particular test will be conducted over a time interval starting at t and ending at t'. During the test, some quantity X (usually a power, light level, or temperature) will be measured at a series of times $t_n = \{t_1, t_2, \ldots t_M\}$ extending from t to t'. These measured quantities will be denoted $X_n \equiv X(t_n)$. The time average of the quantity X is then

$$\langle X \rangle = \frac{1}{M} \sum_{n=1}^{M} X_n \quad , \tag{1}$$

and the time RMS of the quantity is

$$\sigma_X = \sqrt{\frac{1}{M} \sum_{n=1}^{M} \left(X_n - \langle X \rangle \right)^2} \quad . \tag{2}$$

The latter is a measure of the amount of variation in the quantity over the time period. Where a number of different time periods (e.g., days or nights) are under consideration, the average for each may be constructed and identified by a subscript, e.g., for day 1, day 2, etc—in general, day l. It is assumed that time periods for which the averages are compared in this way are all defined in the same way (e.g., from 10PM to 6 AM of each day). The uncertainty in the average calculated in equation 1 due to this time variation (assuming no a priori knowledge of the manner of variation, i.e., that it is random) is

$$\sigma \langle X \rangle = \sqrt{\frac{1}{M(M-1)} \sum_{n=1}^{M} \left(X_n - \langle X \rangle \right)^2} \quad . \tag{2a}$$

In the following, when symbols of the form $\langle X \rangle_l$ and $\sigma \langle X \rangle_l$ occur, they may be assumed to refer to equations 1 and 2a, respectively, for the lth time period.

Cooling & Heating System Efficiency (Tests 4 &5)

It is assumed that data from a number of nights with the chambers all operated normally and an interior air temperature setting of 21ºC is available from previous running of the facility (baseline tests; two such nights will also have been accumulated as part of tests 1 and 2). If there are N such nights available, then we define the mean baseline energy consumption of the chambers as

$$\left(P_\mu\right)_{Base} = \frac{1}{N}\sum_{l=1}^{N} \left\langle P_{C\mu} - P_{H\mu} \right\rangle_l \ , \tag{3}$$

where μ denotes the particular chamber, and $\left\langle P_{C\mu} - P_{H\mu} \right\rangle_l$ denotes the mean value of the measured net power averaged over the lth night. The RMS deviation in this average is defined as

$$\sigma\left(P_\mu\right)_{Base} = \sqrt{\frac{1}{N-1}\sum_{l=1}^{N} \left(\left\langle P_{C\mu} - P_{H\mu} \right\rangle_l - \left(P_\mu\right)_{Base}\right)^2} \ . \tag{4}$$

Outdoor conditions for each night are characterized by evaluating the average outdoor temperature over the same time period used in equation 3 to obtain $\left\langle T_o \right\rangle_l$ for each night, and the overall average and standard deviation of the nighttime mean temperature is calculated from

$$\left\langle\left\langle T_o \right\rangle\right\rangle = \sum_{l=1}^{N} \left\langle T_o \right\rangle_l \ , \tag{5}$$

and

$$\sigma\left\langle T_o \right\rangle = \sqrt{\frac{1}{N-1}\sum_{l=1}^{N} \left(\left\langle T_o \right\rangle_l - \left\langle\left\langle T_o \right\rangle\right\rangle\right)^2} \ . \tag{6}$$

Cooling System Efficiency (Test 4)

The corresponding average outdoor temperature for Test 4, $\left\langle T_o \right\rangle_{T4}$, should be evaluated. $\left\langle T_o \right\rangle_{T4}$ should be within $\sigma\left\langle T_o \right\rangle$ of the overall average mean temperature $\left\langle\left\langle T_o \right\rangle\right\rangle$ above. If there is baseline data for enough nights, nights with $\left\langle T_o \right\rangle_l$ too different from $\left\langle T_o \right\rangle_{T4}$ should be eliminated from the average of equation 3. Define the average power supplied to the (approximately 1500W) co-heater (in chamber μ) during the test as $\left\langle P_{CH\mu} \right\rangle_{T4}$. Then the cooling system efficiency for chamber μ will be

$$\varepsilon_{C\mu} = \frac{\left\langle P_{CH\mu} \right\rangle_{T4}}{\left(\left\langle P_\mu \right\rangle_{T4} - \left(P_\mu\right)_{Base}\right)} \tag{7}$$

The fractional uncertainty in this value can be estimated by

$$\sigma\left(\varepsilon_{C\mu}\right) = \varepsilon_{C\mu} \cdot \sqrt{\left(\frac{\sigma\left\langle P_{CH\mu} \right\rangle_{T4}}{\left\langle P_{CH\mu} \right\rangle_{T4}}\right)^2 + \left(\frac{\left(\sigma\left\langle P_\mu \right\rangle_{T4}\right)^2 + \left(\sigma\left(P_\mu\right)_{Base}\right)^2}{\left(\left\langle P_\mu \right\rangle_{T4} - \left(P_\mu\right)_{Base}\right)^2}\right)} \ , \tag{8}$$

in which the largest term is likely to be due to $\sigma(P_\mu)_{Base}$.

Heating System Efficiency (Test 5)

This test is divided into two time periods, A, when the system is operating in a forced cool/reheat mode with no power to the co-heater ($P_{CH\mu} = 0$), and B, when the coheater is turned on. We calculate the average net power, e.g., $\langle P_\mu \rangle_A = \langle P_{C\mu} - P_{H\mu} \rangle_A$, for each time period and $\langle P_{CH\mu} \rangle_B$ for time period B. Then the cooling system efficiency is

$$\varepsilon_{H\mu} = \frac{\langle P_{CH\mu} \rangle_B}{\left(\langle P_\mu \rangle_B - \langle P_\mu \rangle_A \right)} \quad . \tag{9}$$

One estimate of the uncertainty in this determination can be calculated from the measured uncertainties in the averages,

$$\left(\frac{\sigma(\varepsilon_{H\mu})}{\varepsilon_{H\mu}} \right)_1 = \sqrt{\left(\frac{\sigma \langle P_{CH\mu} \rangle_B}{\langle P_{CH\mu} \rangle_B} \right)^2 + \left(\frac{\left(\sigma \langle P_\mu \rangle_B \right)^2 + \left(\sigma \langle P_\mu \rangle_B \right)^2}{\left(\langle P_\mu \rangle_B - \langle P_\mu \rangle_A \right)^2} \right)} \quad ; \tag{10a}$$

however, this estimate leaves out uncertainty due to possible changes in outdoor conditions between the two time periods. Since test A occurs earlier in the night than test B, it is likely that the average outdoor temperature will be different for the two tests. The effect of this can be estimated by making the same divisions in the baseline data into periods A and B, and calculating the mean power $\langle P_{\mu Base} \rangle_{A,B}$ and mean outdoor temperature $\langle T_{oBase} \rangle_{A,B}$ for each. Then we can define

$$\frac{\Delta \langle P_\mu \rangle}{\Delta \langle T_o \rangle} = \frac{\langle P_{\mu Base} \rangle_B - \langle P_{\mu Base} \rangle_A}{\langle T_{oBase} \rangle_B - \langle T_{oBase} \rangle_B}$$

and use this together with the measured average outdoor temperatures, $\langle T_o \rangle_{A,B}$ from the two parts of Test 5 to make a second uncertainty estimate,

$$\left(\frac{\sigma(\varepsilon_{H\mu})}{\varepsilon_{H\mu}} \right)_2 = \sqrt{\left(\frac{\left(\frac{\Delta \langle P_\mu \rangle}{\Delta \langle T_o \rangle} \cdot \left(\langle T_o \rangle_B - \langle T_o \rangle_A \right) \right)^2}{\left(\langle P_\mu \rangle_B - \langle P_\mu \rangle_A \right)^2} \right)} \quad . \tag{10b}$$

The final uncertainty estimate is then

$$\sigma(\varepsilon_{H\mu}) = \varepsilon_{H\mu} \cdot \sqrt{\left(\left(\frac{\sigma(\varepsilon_{H\mu})}{\varepsilon_{H\mu}}\right)_1\right)^2 + \left(\left(\frac{\sigma(\varepsilon_{H\mu})}{\varepsilon_{H\mu}}\right)_2\right)^2} \quad . \tag{11}$$

Floor, Exterior Wall, and Window UA Values (Tests 1 and 3)

First, use the heating and cooling efficiencies determined above to correct the measured heating and cooling power to give the net power applied to the chamber:

$$P_\mu = \varepsilon_{C\mu} \cdot P_{C\mu} - \varepsilon_{H\mu} \cdot P_{H\mu} \quad , \tag{12}$$

where $P_{C\mu}$ and $P_{H\mu}$ are the measured cooling and heating powers.

In test 1, denote the three chamber temperature settings by L, M and H (low, middle and high). Calculate the averages $\langle P_\mu \rangle$ (using the corrected powers from equation 12), $\langle T_\mu \rangle$ and $\langle T_o \rangle$ for each of the three settings, and fit the data to an equation of the form

$$\langle P_\mu \rangle = A + B\left(\langle T_o \rangle - \langle T_\mu \rangle\right) \ .$$

The data fitted is

$$\begin{Bmatrix} \langle P_\mu \rangle_L & \langle T_\mu \rangle_L & \langle T_o \rangle_L \\ \langle P_\mu \rangle_M & \langle T_\mu \rangle_M & \langle T_o \rangle_M \\ \langle P_\mu \rangle_H & \langle T_\mu \rangle_H & \langle T_o \rangle_H \end{Bmatrix} \ .$$

(This is equivalent to doing a linear regression, e.g., in Excel.) Denote the value of B obtained for chamber μ by $B_{1\mu}$. Then in the notation of reference [1]

$$B_{1\mu} = A_{T\omega_\mu} \cdot U_{\omega_\mu} + \sum_{k=floor,extwall} A_{\mu k} \cdot U_{\mu k} \quad . \tag{13}$$

In Test 3, let the thermal resistance of the added foam insulation be denoted $R_{I\mu}$. If the above procedure is repeated for the Test 3 data to determine a new value of the constant B, $B_{3\mu}$, then

$$B_{3\mu} = A_{T\omega_\mu} \cdot \frac{1}{\frac{1}{U_{\omega_\mu}} + R_{I\mu}} + \sum_{k=floor,extwall} A_{\mu k} \cdot U_{\mu k} \tag{14}$$

under the assumption that adding the foam does not change the interior convective or radiative conditions, and that the exterior conditions in the two tests are comparable.

These assumptions, although not necessarily good, are necessary for a simple analysis of the tests. One can solve equations 13 and 14 to obtain a value for U_{ω_μ},

$$U_{\omega_\mu} = \frac{\left(B_{1\mu} - B_{3\mu}\right)}{2A_{T\omega_\mu}}\left(1 + \sqrt{1 + 4\frac{A_{T\omega_\mu}}{R_{I\mu}\cdot\left(B_{1\mu} - B_{3\mu}\right)}}\right) \tag{15}$$

and this value can be substituted back into equation 13 to obtain

$$\sum_{k=\,floor,extwall} A_{\mu k}\cdot U_{\mu k} = B_{1\mu} - \frac{\left(B_{1\mu} - B_{3\mu}\right)}{2}\left(1 + \sqrt{1 + 4\frac{A_{T\omega_\mu}}{R_{I\mu}\cdot\left(B_{1\mu} - B_{3\mu}\right)}}\right) \tag{16}$$

Ceiling & Interior Wall UA Values (Test 2)

This analysis follows the same procedure as the above analysis for the window and floor/exterior walls, except that the equation fitted is of the form

$$\left\langle P_\mu \right\rangle = A + B\left(\left\langle T_G \right\rangle - \left\langle T_\mu \right\rangle\right)$$

And the data set to be fitted is

$$\begin{Bmatrix} \left\langle P_\mu \right\rangle_L & \left\langle T_\mu \right\rangle_L & \left\langle T_G \right\rangle_L \\ \left\langle P_\mu \right\rangle_M & \left\langle T_\mu \right\rangle_M & \left\langle T_G \right\rangle_M \\ \left\langle P_\mu \right\rangle_H & \left\langle T_\mu \right\rangle_H & \left\langle T_G \right\rangle_H \end{Bmatrix} .$$

In making up this data set, attention should be paid to the values of $\left\langle T_o \right\rangle_L$, $\left\langle T_o \right\rangle_M$ and $\left\langle T_o \right\rangle_H$. If these are too different from the corresponding values of $\left\langle T_\mu \right\rangle$, then the results of the above section on the exterior surfaces should be used to correct the values of $\left\langle P_\mu \right\rangle$ for the variations. However, this may not be the best way to make such corrections; see below.

The value of the slope constant obtained, $B_{2\mu}$, is a direct measure of the effective UA value of all the chamber envelope elements that face onto the guard:

$$B_{2\mu} = \sum_{k\neq\,floor,extwall} A_{\mu k}\cdot U_{\mu k} \tag{17}$$

Sensitivity To Changes in Static Conditions (Tests 6,7 and 8)

The chamber temperature control system responds to the temperature of the chamber air, and delivers its control energy (cooling or heating) directly to the chamber air in the form of flows of air colder or warmer than that of the chamber. However, lights and occupants

deliver power to the chamber both in the form of direct heating of the chamber air (by warm surfaces and, in the case of occupants, by evaporation of perspiration) and in the form of radiant fluxes, which only affect the chamber air by raising the temperatures of surfaces in which they are absorbed. Some of this energy flow absorbed in chamber surfaces may flow out through the chamber envelope and never appear as a change in the chamber power; some may also be stored in the envelope (or in interior thermal mass such as furniture) and affect the chamber power at a time later than the occurrence of the radiant flux. Test 6 and 7 examine the first of these two effects.

In Test 6 there is a radiant co-heater, and the radiant output power, $Q_{R\mu}$ will be some fraction x_μ of the applied power,

$$Q_{R\mu} = x_\mu \cdot \left(P_{CH\mu}\right)_{T\,6} \tag{18}$$

A separate measurement on the radiant heater for chamber μ would be needed to determine x_μ. Initially, we assume that $x_\mu = 1$. If the radiant flux affected the chamber in exactly the same way as convective heating, then this test would simply be a repeat of Test 4, and (since the power has already been corrected for the efficiency determined in that test, the change in power above the pre-test (nighttime) baseline would be

$$\left\langle P_\mu \right\rangle - \left(P_\mu\right)_{Base} = \left\langle P_{CH\mu} \right\rangle_{T6}$$

so that we can define a radiative sensitivity,

$$\frac{d\left\langle P_\mu \right\rangle}{dQ_{R\mu}} = \frac{\left\langle P_\mu \right\rangle_{T\,6} - \left\langle P_{CH\mu} \right\rangle_{T\,6} - \left(P_\mu\right)_{Base}}{Q_{R\mu}} \tag{19}$$

and by estimating changes average radiative flux the resultant changes in average chamber power can be estimated. Note that in the test the radiant flux was arranged so that it was not directly incident on the window, so that equation 19 is primarily due to the non-window envelope (although the window participates throught multiple reflections of the radiation and by long-wavelength radiative coupling).

The first part of Test 7 repeats this determination for lighting. For a given lighting power level in chamber μ, L_μ, the radiant flux will be

$$Q_{L\mu} = y_\mu \cdot \mathrm{L}_\mu \ .$$

In general, y_μ will not be equal to one. It is best determined from the lamp specifications or data supplied by the lamp manufacturer. It could be estimated by radiant flux measurements made in the chamber, but this will be complicated by interreflections. The lighting radiative sensitivity is then

$$\left(\frac{d\langle P_\mu\rangle}{dQ_{L\mu}}\right)_{Tot} = \frac{\langle P_\mu\rangle_{T7A} - \langle P_{CH\mu}\rangle_{T7A} - (P_\mu)_{Base}}{Q_{L\mu}} \tag{20}$$

In the first part of the test (the first night, denoted T7A) part of the light flux falls on the window, and will be transmitted out of the chamber. Equation 20 therefore does not characterize the non-window envelope as does equation 19. The second part (T7B) of the test (approximately) corrects for this by placing opaque insulation over the window. We can characterize the resulting sensitivity determined from this test as that of the "shell", i.e., the non-window envelope, analogous to equation 19:

$$\left(\frac{d\langle P_\mu\rangle}{dQ_{L\mu}}\right)_{Shell} = \frac{\langle P_\mu\rangle_{T7B} - \langle P_{CH\mu}\rangle_{T7B} - (P_\mu)_{Base}}{Q_{L\mu}} \tag{21}$$

In Test 8 we denote the normal air flow rate by $f_{R\mu}$ and the reduced flow rate by $f_{R\mu} - \Delta f_\mu$. If the two tests are distinguished by the subscripts T8A (at the normal flow rate) and T8B (at the reduced flow rate), then we define

$$\mathbf{F}_\mu = \frac{\langle P_\mu\rangle_{T8B} - \langle P_\mu\rangle_{T8A}}{\Delta f_\mu} \tag{22}$$

Dynamic Tests

Chamber Temperature Ramp (Test D1)

Dynamic Test 1 (D1) is intended to measure the effect of heat storage in the chamber envelope, but will also give considerable information about the performance of the control system. In this test, beginning at a time t_1 a ramp of the interior temperature with time at a constant rate $\frac{dT_\mu}{dt}$ is simulated by advancing the temperature set point by a fixed amount each minute until a time t_2, after which the interior temperature set point is decreased by the same amount each minute (simulating a constant rate $-\frac{dT_\mu}{dt}$) until at a time $t_3$the set point has returned to its original setting, at which time the set point is kept constant. The idealized response of the chamber power to these actions is shown in Figure 1. This idealized response is described by the equation

$$P_\mu(t) = \begin{cases} P_1 & t \le t_1 \text{ or } t \ge t_3 \\ P_1 + \Delta P + B\cdot(t - t_1) & t_1 \le t \le t_2 \\ P_1 - \Delta P + B\cdot(2t_2 - t_1 - t) & t_2 \le t \le t_3 \end{cases} . \tag{23}$$

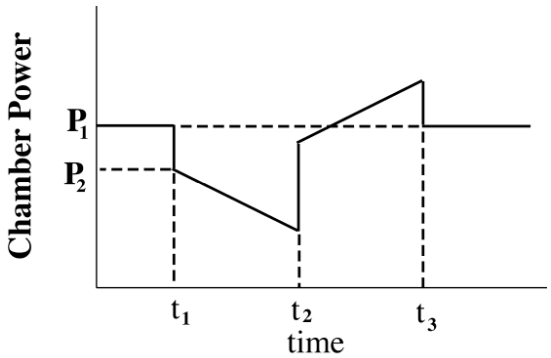

Figure 1. Idealized response of the chamber power.

If the observed response remotely resembles this curve, then equation 23 can be fit to the data (consisting of the time series of P_μ) to obtain the constants $(\Delta P)_{D1\mu}$ and $B_{D1\mu}$ (where the subscripts D1 and μ have been added to identify the test and the chamber, respectively). From the constant $(\Delta P)_{D1\mu}$ the effective heat capacity of the chamber, $C_{\mu Eff}$, can be extracted:

$$C_{\mu Eff} = \frac{(\Delta P)_{D1\mu}}{\left|\frac{dT_\mu}{dt}\right|} \tag{24}$$

while the constant $B_{D1\mu}$ provides a check on the method, since

$$B_{D1\mu} = -\left(A_{T\omega_\mu} \cdot U_{\omega_\mu} + \sum_{k=floor,extwall} A_{\mu k} \cdot U_{\mu k} + \sum_{k \neq floor,extwall} A_{\mu k} \cdot U_{\mu k} \right) \cdot \left|\frac{dT_\mu}{dt}\right| \tag{25}$$

and the terms in parentheses on the right hand side of equation 25 have been determined in Tests 1 and 2.

There are several ways in which the measured data might be expected to differ from the ideal curve in Figure 1.

1. Because the data has a the short averaging period produced by the measurement system rather than the long one of the static tests , variations in the outdoor temperature may cause the baseline (the dashed horizontal line at the value P_1 in Figure 1) to have a slope. This can be corrected for by first fitting a straight line to this baseline (the data before and long after the test), and correcting the data for this slope prior to undertaking the above analysis.
2. The fact that the test is carried out in discrete steps of the setpoint temperature rather than a continuous variation may result in a “stairstep” shape to the curve, possibly with oscillations at each step caused by the control system response.

Both of the above are cases where the deviations from the ideal curve are such that the model of equation 23 may still be fit to the data. It is also possible that the measured data will not resemble the ideal curve in any way. This would be an indication that the response of the control system is very different from that assumed for the ideal curve, and would indicate that more information about the control system response needs to be obtained.

It is also possible that after fitting the data to equation 23, equation 25 is found not to hold. This indicates that a static treatment of the heat flow through the chamber envelope is inadequate, and a more detailed model that takes into account the envelope response time is needed. This result would also call into question the simplified analysis of static tests 1, and 2.

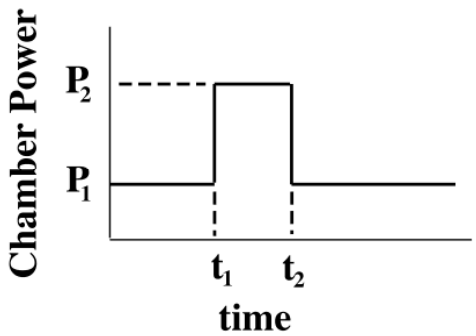

Figure 2. Ideal response curve.

Control System Response (Test D2)

This test examines the time response of the control system to variations in the chamber load. The ideal response curve is shown in Figure 2. The measured curve can be expected to deviate from this, and the nature of the deviation will give information about the response, especially the response time, of the control system.

The data before the time t_1 of the onset of the heating pulse (indicated in Figure 2) and after t_3, a time taken sufficiently long after the time t_2 in the figure, should be fit to a straight line to determine the base level for the test, $\left(P_\mu\right)_{Base} = P_0 + B \cdot t$. The heater power averaged over the period $\left(t_1, t_2\right)$ is denoted $\left\langle P_{CH\mu} \right\rangle_{D2}$. If we denote by $\left\langle P_\mu \right\rangle_t$ the average of the chamber net power taken over the interval $\left(t_1, t\right)$, then we determine t from the requirement that it be correspond to the shortest such interval for which

$$\left\langle P_\mu \right\rangle_t = \left\langle P_{CH\mu} \right\rangle_{D2} + \left\langle \left(P_\mu\right)_{Base} \right\rangle_t \tag{26}$$

This interval ($t - t_1$) represents the minimum length of time over which the chamber power must be averaged to produce meaningful results.

Radiant Heater Pulse Test (D3)

This test measures the average response to a radiant flux. As above, define a baseline power level, and let the average of the applied heater power over the interval (t_1, t_2) be $\langle P_{CH\mu} \rangle_{D3}$. As in equation 18, there will be a radiant flux:

$$\langle Q_{R\mu} \rangle = x_\mu \cdot \langle P_{CH\mu} \rangle_{D3} \tag{27}$$

where as before we initially assume $x_\mu = 1$, although a separate measurement would give a more accurate result to this analysis. Then

$$\mathcal{V}_\mu^S = \frac{\langle P_\mu \rangle_t - \left(\langle P_{CH\mu} \rangle_{D3} + \langle (P_\mu)_{Base} \rangle_t \right)}{\langle Q_{R\mu} \rangle} \tag{28}$$

where we have taken $Q_{R\mu}$ to mimic the effects of transmitted solar radiation.

Lighting Pulse (Test D4)

This test is a repeat of the above test using a light pulse rather than a radiant heat pulse, but otherwise the analysis is carried out in the same way. The radiant fraction of the lighting energy is

$$\langle Q_{L\mu} \rangle = y_\mu \cdot \langle \mathrm{L}_\mu \rangle \tag{29}$$

and we initially assume $y_\mu = 1$. We then calculate the sensitivity to lighting energy by

$$\mathcal{V}_\mu^{\mathcal{L}} = \frac{\langle P_\mu \rangle_t - \left(\langle \mathcal{L}_\mu \rangle_{D3} + \langle (P_\mu)_{Base} \rangle_t \right)}{\langle Q_{L\mu} \rangle} \tag{30}$$

Radiant and Light Losses Through Window (Tests D5, D6)

Radiant energy absorbed by the window may be transferred as heat to the out-of-doors without appearing in the measurement of chamber net power. The same is true for absorbed light, but in addition the window will transmit a fraction of light incident on its interior surface. The same may be true of radiant energy in the heater pulse test, depending on the spectrum produced by the quartz heater. Therefore, for these tests the analysis for Tests D3 and D4 should be repeated, and differences in the result examined. At the simplest level of analysis, uncertainties should be assigned to the $\mathcal{V}_\mu^{\mathcal{L}}$ and $\mathcal{V}_\mu^S$ values as follows:

$$\sigma(\mathcal{V}_\mu^{\mathcal{L}}) = \left|(\mathcal{V}_\mu^{\mathcal{L}})_{D4} - (\mathcal{V}_\mu^{\mathcal{L}})_{D6}\right| \tag{30}$$

$$\sigma\left(\mathcal{V}_\mu^{S}\right) = \left|\left(\mathcal{V}_\mu^{S}\right)_{D3} - \left(\mathcal{V}_\mu^{S}\right)_{D5}\right| \tag{31}$$

where the subscripts denote the values obtained in the analysis of the various dynamic tests.

Application of the Corrections

Energy savings in the testbed measurements are defined [2] as

Energy savings = Base case energy use – Test case energy use ± Adjustments. (32)

This corresponds to a measurement of the average power in two chambers, one, denoted B, represents the base case, and the other, denoted T, represents the test case. If we denote with the subscript M (for measured) the "raw" energy savings without the adjustment term above, in the present notation equation 32 reads

$$(\Delta P_{BT})_M = \langle P_B \rangle - \langle P_T \rangle \tag{33}$$

It will generally be the case that the window solar transmittances $\mathcal{T}_B$ and $\mathcal{T}_T$, and the lighting powers L_B and L_T will be different for the two chambers—that is the point of the test. Other quantities may also differ: interior temperature, effective guard temperature, air flow rate. It is assumed that the intended chamber interior temperature is T_R, and the intended guard temperature is T_{G0}. We denote the actual chamber temperature, guard temperature, and air flow rate by T_B, T_{GB} and f_B, respectively, for the base case chamber and by T_T, T_{GT} and f_T for the test case chamber. Then (denoting the corrected net power by dropping the M subscript)

$$\begin{aligned}
\Delta P_{BT} = {} & \langle P_B \rangle - \langle P_T \rangle - \left(\mathbf{S}_B^{\omega} + \mathbf{S}_B^{F} + \mathbf{S}_B^{G}\right) \cdot \langle T_R - T_B \rangle + \left(\mathbf{S}_T^{\omega} + \mathbf{S}_T^{F} + \mathbf{S}_T^{G}\right) \cdot \langle T_R - T_T \rangle \\
& - \mathbf{S}_B^{G} \cdot \langle T_{GB} - T_{G0} \rangle + \mathbf{S}_T^{G} \cdot \langle T_{GT} - T_{G0} \rangle \\
& - \left(\mathbf{S}_B^{\omega} - \mathbf{S}_T^{\omega}\right) \langle T_o - T_R \rangle - \left(\mathbf{S}_B^{G} - \mathbf{S}_T^{G}\right) \cdot \langle T_{G0} - T_R \rangle - \left(\mathbf{S}_B^{F} - \mathbf{S}_T^{F}\right) \cdot \langle T_o - T_R \rangle \\
& - \mathbf{F}_B \cdot \langle f_B - f_0 \rangle + \mathbf{F}_T \cdot \langle f_T - f_0 \rangle \\
& - \mathcal{V}_B^{S} \cdot \langle \mathcal{T}_B S \rangle + \mathcal{V}_T^{S} \cdot \langle \mathcal{T}_T S \rangle - \mathcal{V}_B^{L} \langle \mathcal{L}_B \rangle + \mathcal{V}_T^{L} \langle \mathcal{L}_T \rangle
\end{aligned} \tag{34}$$

It must be noted that the average measured powers have been corrected for efficiency using equation 12.

IV. Thermal Calibration Results

Introduction

The Lighting Testbed Facility is a building consisting of three identical rooms, each surrounded on three sides and above by a guard space where conditioned air is circulated. The rooms have an insulated floor above a crawl space ventilated to the out of doors, and the fourth (south-facing) side of each room consists of an opening to the outdoors into which a selected fenestration system is installed. A general description of the facility, its monitoring protocols and detailed design have been given in separate reports.(Facilities Division 2003; Lee, DiBartolomeo et al. 2003; Lee, DiBartolomeo et al. 2003)

The general intended use of the facilty is to study the performance of electrochromic and other dynamically controlable fenestrations. One part of this is to compare the thermal loads resulting from different fenestrations or control strategies. To do this it is necessary to account for heat flows that result from differences among the rooms that are irrelevant to the fenestration comparisons. Since the rooms were built with standard construction techniques, some differences in thermal properties are expectable. In addition, each is separately controlled by control systems that are less than perfect, and conditioned air is supplied to each by separate duct systems. This means that there are likely to be differences in the internal air temperatures of the rooms, even when they are nominally set to the same temperature. In addition, duct losses between the point where applied heating or cooling is measured and the entrance to the test room could differ from room to room, and there could be miscalibrations of the measurement apparatus. The purpose of the calibration is to determine the magnitude of these differences, and, where possible, to correct for them.

Steady-State Correction Model

The basic thermal quantity measured is the net chamber power, P_0, where ($\mu = a,b,c$ denotes the particular room; see Nomenclature section for notation)

$$P_\mu = \varepsilon_\mu \mathcal{C}_\mu - \eta_\mu \mathcal{H}_\mu - \mathcal{L}_\mu - \mathcal{F}_\mu - \mathcal{P}_\mu \tag{1}$$

where the constants ε_μ and η_μ are inserted to account for the possibility that the measured cooling and heating powers may not represent the actual power removed from or added to the chamber. We assume that all quantities are averaged over a time period suitably long compared to the response times of the control systems, and define a steady-state heat transfer model of the effects of temperature changes on the rooms:

$$P = P_0 + UAW \cdot (T_E - T_I) + UAF \cdot (T_U - T_I) + UAG \cdot (T_G - T_I). \tag{2}$$

The chamber air is recirculated through ducts which contain a heater and a cooling coil. The measured heating power is the wattage applied to this duct heater, and the measured

cooling power is calculated from the fluid flow and temperature increase through the coil. The devices making these measurements could be less than perfectly calibrated, or there could be power losses in the ducts. These possibilities are accounted for by the constants ε_μ and η_μ. In addition, the temperature sensors measuring the fluid temperature gain could have an offset. This possibility is accounted for by inclusion of the offset term P_0 in equation (2).

In order to determine the four parameters in this model a series of static tests were conducted. First the test room and guard temperatures were simultaneously set to 14ºC, 21ºC (the normal operating point) and 31ºC for a minimum of one day each with the net power measured during each test. Next, the room air temperatures were set to 16ºC, which approximated the average outdoor nighttime temperature, and the guard temperatures were stepped over the same intervals. Finally, the window walls were covered with insulation and the room and guard air temperatures again stepped over the three temperatures.

In the initial analysis of these tests the heating and cooling calibration constants were not known, so a provisional net power P_μ^M was used, which is the net power calculated from equation (1) assuming a value of 1 for ε_μ and η_μ. It can be shown that use of the provisional net power could also result in changing the value of the intercept term in eqn 2.

Fits to The Static Test Data

Fitting the test data to equation (2) is complicated by the fact that it is not possible to control either T_E or T_U. This means that in fitting the data the constants UAW and UAF will be strongly correlated. We handled this by first calculating UAF based on the chamber dimensions and the design of the floor structure. UAF was held constant at this value (2.12 W/K) and equation 2 was fit to the test data without window insulation to determine preliminary values of UAW, UAG and P_0. These are shown in Table 1. Next, these values were held constant and the model fitted to the tests that had insulation over the window to determine a new value for UAF. In these tests, equation (2) had to be modified to replace UAW with the expression $UAW\ /(1+r)$, where r is the ratio of the thermal resistance of the added insulation to the effective resistance of the window/frame/wall combination without the insulation. This was taken to be $\frac{1}{UAW}$, and the value obtained in the first fit was used. The resulting value of r (4.8) was considered to be constant in all subsequent analysis. Finally, this new value of UAF was fixed and all the data (including the insulated window tests, for which the modified expression involving UAW was used) was again fit to determine final values of UAW, UAG, and P_0. The parameter values obtained are shown in Table 2. The errors listed in the table are derived by standard methods (Press, Teukolsky et al. 1992), and correspond to one standard deviation.

As can be seen from the two tables, the final values of the parameters differ from the initial ones by less than the error of the final values. In particular, the value of UAF for all three chambers is consistent with the initial calculated value, within errors. Nor is there persuasive evidence for chamber-to-chamber differences, with the exception of the

values of P_0. For P_0 the values for different chambers are in some cases significantly different, for example, that for room a is around three standard errors smaller than that for room b.

It is difficult to display graphically a fit in three independent variables. In Figures 1-9 we utilize three one-variable graphs for each of the three rooms. In Figure 1, measured power is plotted against $(T_E - T_I)$ for all the tests in which T_I was varied. The measured points in this figure have been corrected to a zero value of the other two temperature differences, i.e., the measured power plotted is

$$P^{PLOT} = P - UAF \cdot (T_U - T_I) - UAG \cdot (T_G - T_I)$$

while the fitted power plotted is

$$P = P_0 + UAW \cdot (T_E - T_I)$$

for the uninsulated window and

$$P = P_0 + \frac{UAW}{1+r} \cdot (T_E - T_I)$$

for the tests with the window covered with insulation. A similar proceure was followed for the plot of power against the other two temperature differences in Figures 2 and 3.

Determination of the Heating and Cooling Calibration Constants

The constants ε and η were determined by co-heating, placing a large-capacity convective heater in each chamber, measuring its power input, and observing its effect on the measured heating and cooling power.

In the case of the cooling power, this was fairly simple. Additional heat applied to the chamber causes the control system to increase the average cooling power. There were complications caused by the solar gain, since these tests were not conducted with the window insulation in place, but by midnight the effects of the solar gain are gone and it was possible to interpret the test, using equation (2) to correct for the heat flows caused by the outdoor and guard temperatures.

For the heating power, it was necessary to force the cooling power up by manually setting its controlling fan, such that there was also a heating power greater than the power of the heater . When the heater was run this heating power then was decreased by the action of the control system, and one could determine η by the amount of this decrease.

The results of these measurements are shown in Table 3. For both room b and room c both constants are quite consistent with a value of one, being within one standard error unit of that value. For room a the values differ from one by more than one standard error, but less than two. So for none of the rooms is there firm evidence for a calibration constant different from one. The error values are around 3%. To this level of accuracy, then, $\varepsilon = 1$ and $\eta = 1$ were assumed for all three chambers.

These tests always use differences in the cooling power, and so would not detect an offset. This remains a possible interpretation for the fitted values of P_0.

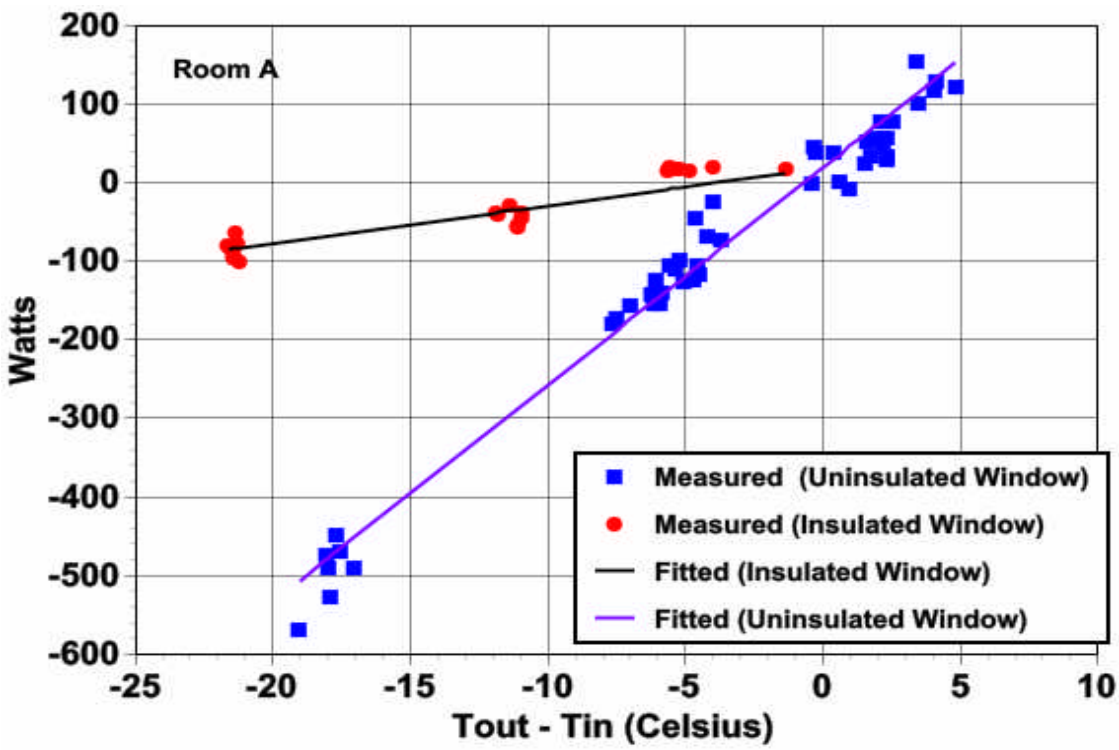

Figure 1. Fitting the Tests Determining UAW, Room A. The plotted data points have been corrected (using the fitted values of UAF and UAG) to zero values of all the temperature differences in equation (2) other than the one displayed. The fitted lines are equation (2) with these temperature differences set to zero.

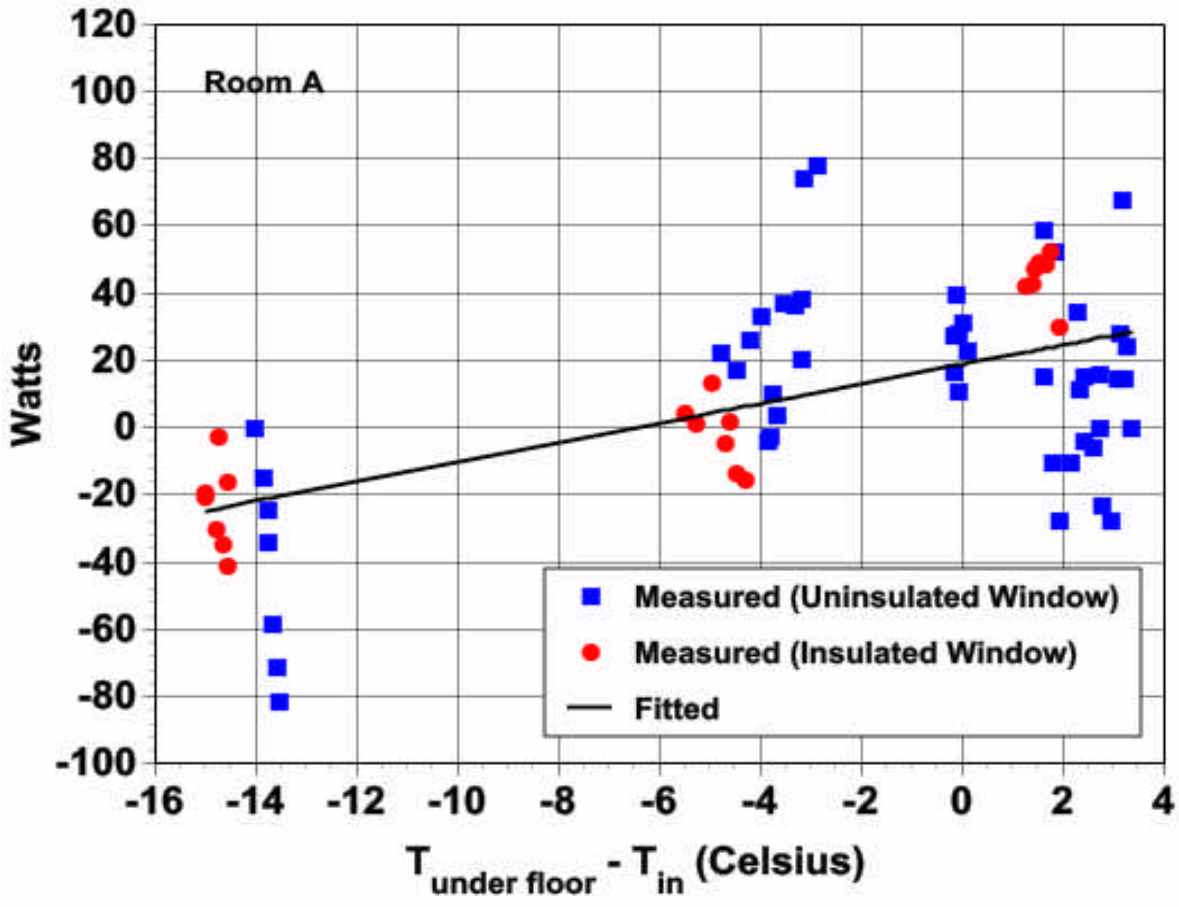

Figure 2. Fitting the Tests Determining UAF, Room A. The plotted data points have been corrected (using the fitted values of UAW and UAG) to zero values of all the temperature differences in equation (2) other than the one displayed. The fitted lines are equation (2) with these temperature differences set to zero. The value of UAF was obtained using only the measured points for the insulated window; the others are included for information.

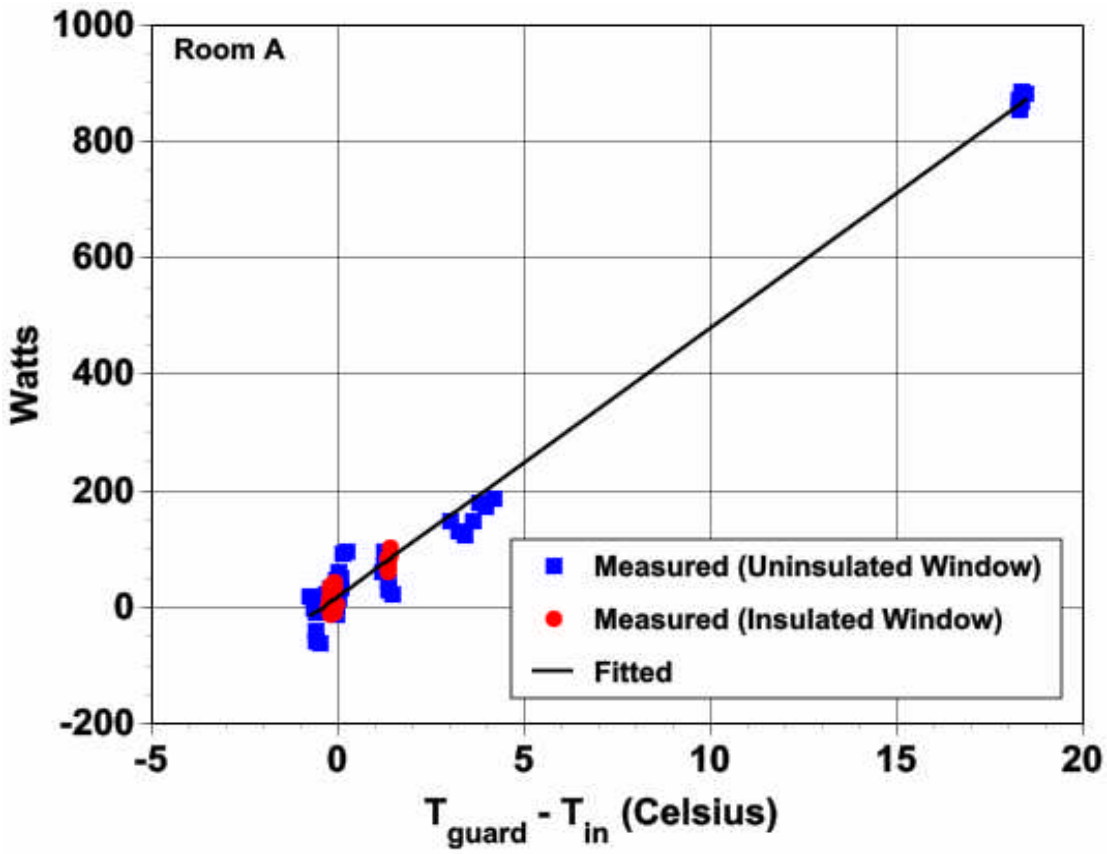

Figure 3. Fitting the Tests Determining UAG, Room A. The plotted data points have been corrected (using the fitted values of UAW and UAF) to zero values of all the temperature differences in equation (2) other than the one displayed. The fitted lines are equation (2) with these temperature differences set to zero.

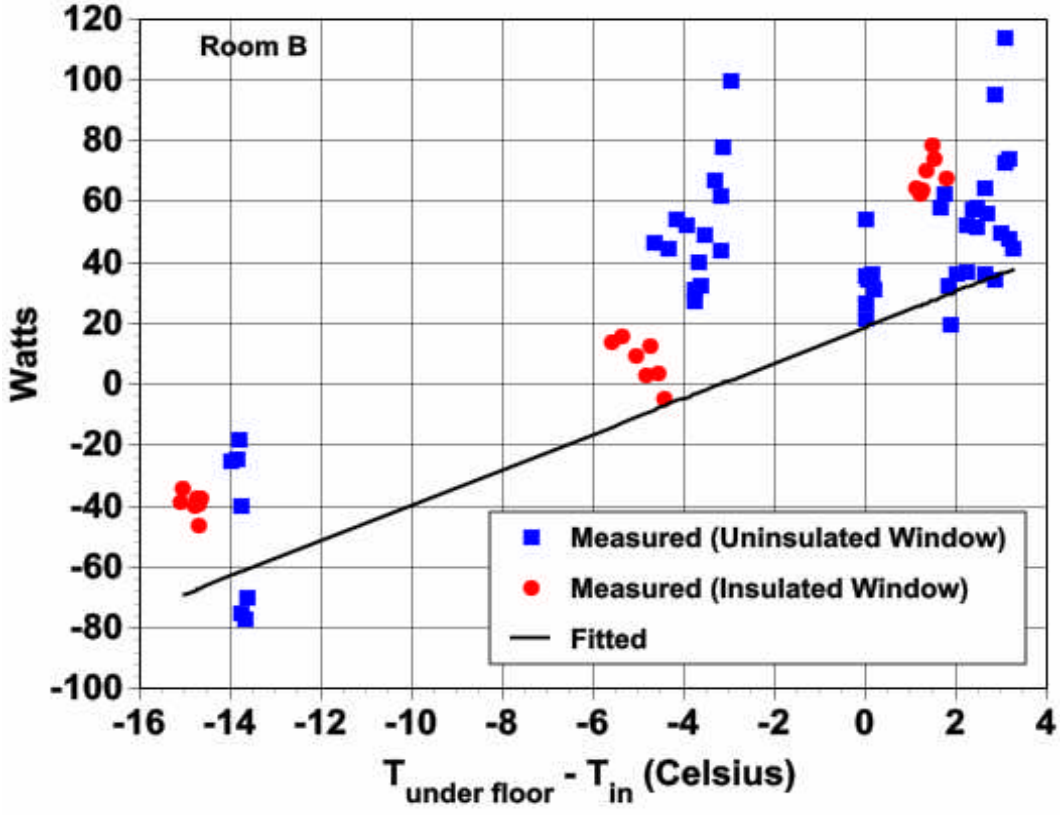

Figure 4. Fitting the Tests Determining UAW, Room B. The plotted data points have been corrected (using the fitted values of UAF and UAG) to zero values of all the temperature differences in equation (2) other than the one displayed. The fitted lines are equation (2) with these temperature differences set to zero.

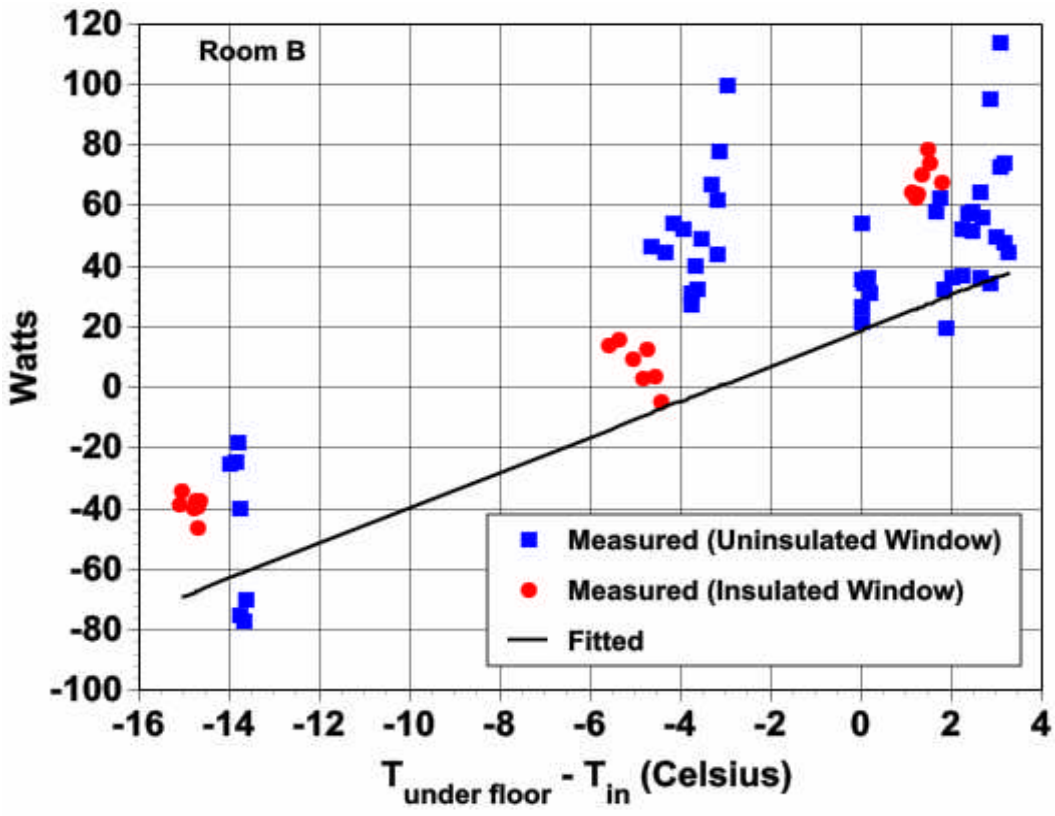

Figure 5 Fitting the Tests Determining UAF, Room B. The plotted data points have been corrected (using the fitted values of UAW and UAG) to zero values of all the temperature differences in equation (2) other than the one displayed. The fitted lines are equation (2) with these temperature differences set to zero. The value of UAF was obtained using only the measured points for the insulated window; the others are included for information.

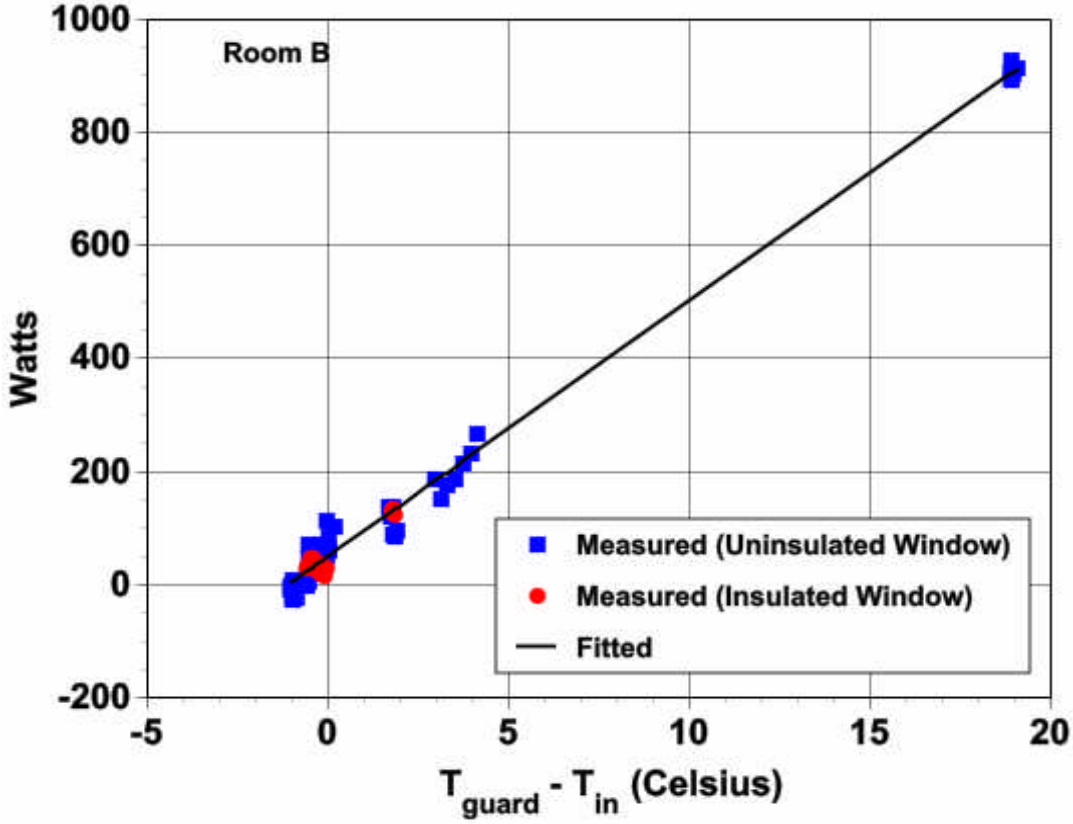

Figure 6 Fitting the Tests Determining UAG, Room B. The plotted data points have been corrected (using the fitted values of UAW and UAF) to zero values of all the temperature differences in equation (2) other than the one displayed. The fitted lines are equation (2) with these temperature differences set to zero.

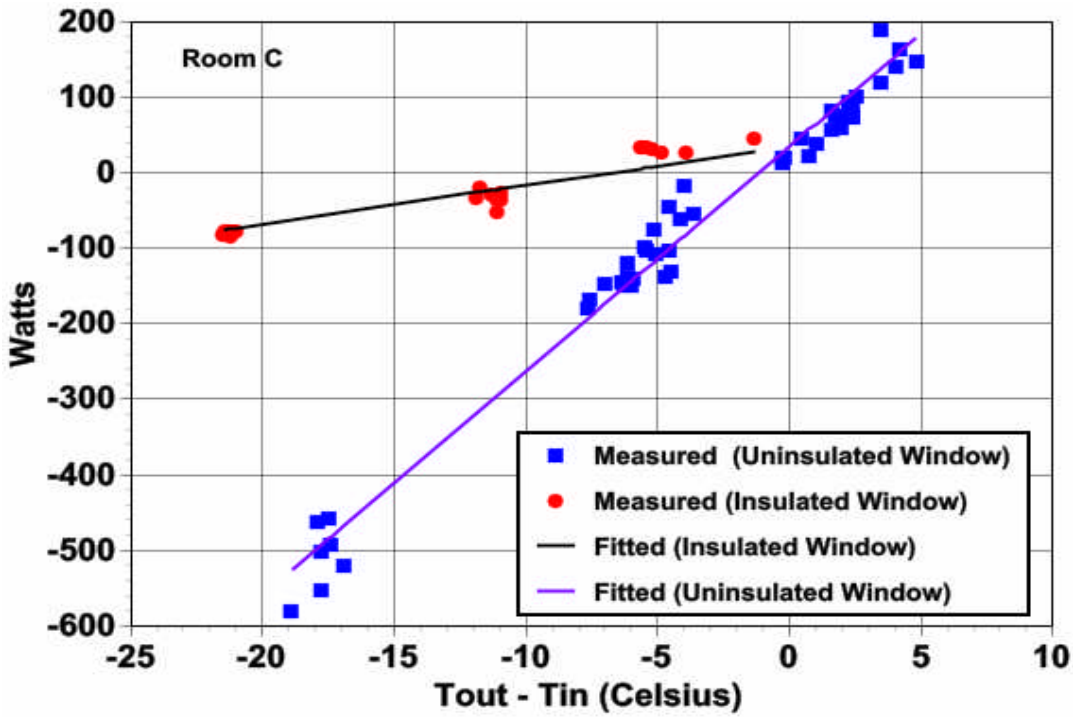

Figure 7 Fitting the Tests Determining UAW, Room C. The plotted data points have been corrected (using the fitted values of UAF and UAG) to zero values of all the temperature differences in equation (2) other than the one displayed. The fitted lines are equation (2) with these temperature differences set to zero.

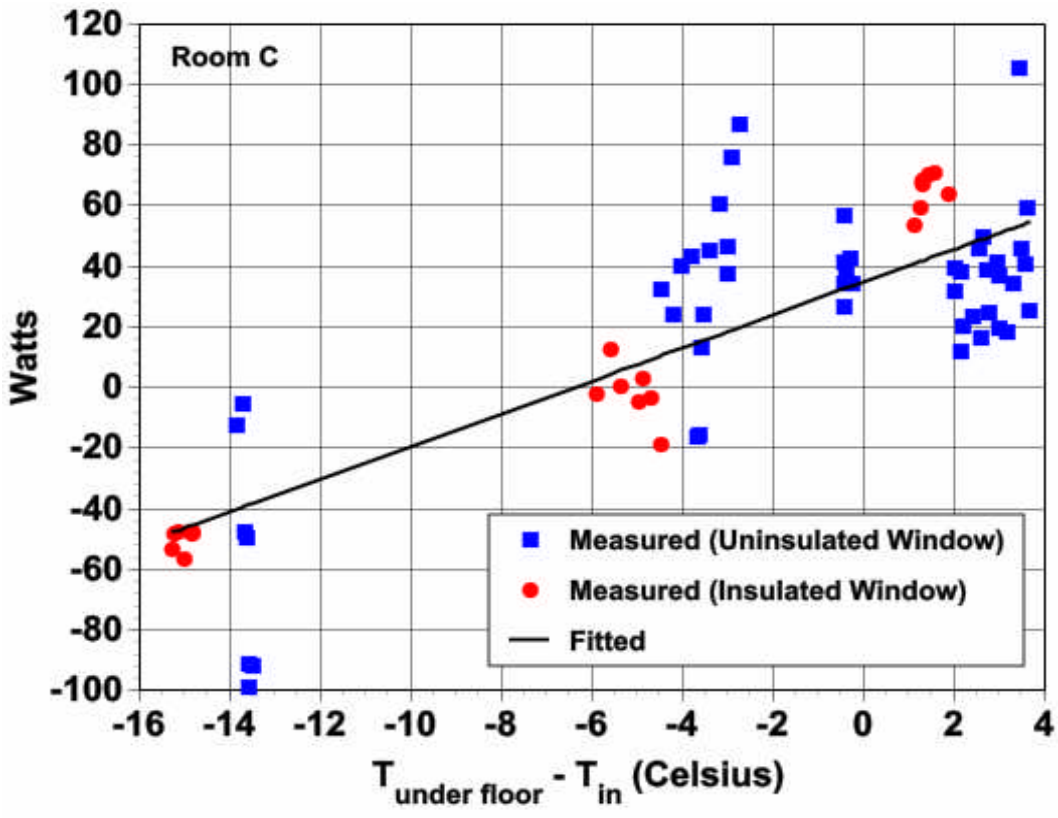

Figure 8 Fitting the Tests Determining UAF, Room C. The plotted data points have been corrected (using the fitted values of UAW and UAG) to zero values of all the temperature differences in equation (2) other than the one displayed. The fitted lines are equation (2) with these temperature differences set to zero. The value of UAF was obtained using only the measured points for the insulated window; the others are included for information.

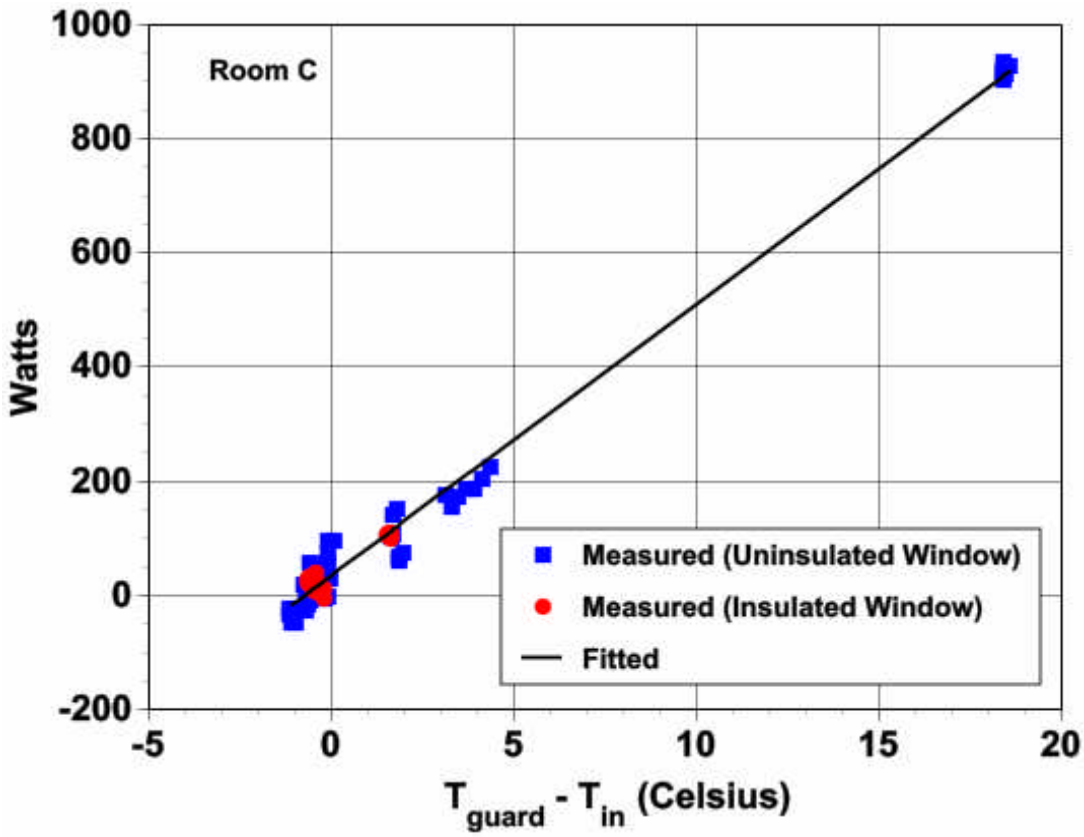

Figure 9 Fitting the Tests Determining UAG, Room C. The plotted data points have been corrected (using the fitted values of UAW and UAF) to zero values of all the temperature differences in equation (2) other than the one displayed. The fitted lines are equation (2) with these temperature differences set to zero.

Table 1. Results from the Initial Fit to the Static Tests

	UA Window	UA Floor	UA Guard	Power Offset
	Fitted	(Assumed)	Fitted	Fitted
Room	W/K	W/K	W/K	Watts
A	28.05	2.12	46.43	15.74
B	28.98	2.12	45.88	54.02
C	32.25	2.12	48.26	35.42

	UA Window		UA Floor		UA Guard		Power Offset	
	Value	Error	Value	Error	Value	Error	Value	Error
Room	W/K	W/K	W/K	W/K	W/K	W/K	Watts	Watts
A	27.60	2.26	2.90	2.89	46.10	0.98	18.69	7.97
B	25.94	1.89	5.84	2.39	45.14	0.78	50.22	6.66
C	29.68	2.41	5.40	3.00	47.50	0.92	34.63	8.24

Table 2. Results From The Final Fit To The Static Tests

	Heating Calibration Constant			
			99% Confidence Limits	
	Best -fit Value	Error	Lower	Upper
Room A	1.06	0.03	0.96	1.16
Room B	1.02	0.03	0.94	1.10
Room C	1.06	0.03	0.97	1.16
	Cooling Calibration Constant			
			99% Confidence Limits	
	Best -fit Value	Error	Lower	Upper
Room A	0.96	0.03	0.88	1.05
Room B	1.02	0.03	0.94	1.10
Room C	1.00	0.04	0.90	1.10

Table 3.

Nomenclature

Subscripts:

μ	General room subscript
0	Denotes a constant or initial condition
I	Interior air
G	Guard air
U	Underfloor air
E	Exterior air
a, b, c	Room subscripts; denote particular rooms

Superscripts:

M	Measured

Symbols:

P	Net room (or chamber) power
$\mathscr{C}$	Measured energy extracted by the cooling system
$\mathscr{H}$	Measured heat added by the heating system
$\mathscr{L}$	Lighting power
$\mathscr{F}$	Fan power
$\mathscr{P}$	In-room electric ("plug") power
ε	Cooling system calibration constant
η	Heating system calibration constant
T	Temperature
ΔT	Temperature difference
UAF	Effective heat transfer coefficient (heat flow/unit temperature difference) for floor
UAW	Effective heat transfer coefficient for wall containing window
UAG	Effective heat transfer coefficient between room and guard space
$\langle X \rangle$	Average value of the quantity X
R	Thermal resistance
r	Ratio of two thermal resistances

References

Facilities Division, L. (2003). B71H Window Test Facility, Lawrence Berkeley National Laboratory.

Lee, E., D. DiBartolomeo, et al. (2003). Testbed Design Specifications: Engineering Field Tests Using a Full-Scale Testbed Facility, Lawrence Berkeley National Laboratory.

Lee, E., D. DiBartolomeo, and J. Klems (2003). Engineering Field Tests Using A Full-scale Testbed Facility: Energy Monitoring Protocol. Lawrence Berkeley National Laboratory, Draft Report 4/30/03.

Press, W. H., S. A. Teukolsky, et al. (1992). Numerical Recipes in Fortran. New York, Cambridge University Press.